

Nys-Curve: Nyström-Approximated Curvature for Stochastic Optimization

Hardik Tankaria², Dinesh Singh¹, Makoto Yamada^{1,2}

¹RIKEN AIP, ²Kyoto University,

October 19, 2021

Abstract

The quasi-Newton methods generally provide curvature information by approximating the Hessian using the secant equation. However, the secant equation becomes insipid in approximating the Newton step owing to its use of the first-order derivatives. In this study, we propose an approximate Newton step-based stochastic optimization algorithm for large-scale empirical risk minimization of convex functions with linear convergence rates. Specifically, we compute a partial column Hessian of size $(d \times k)$ with $k \ll d$ randomly selected variables, then use the *Nyström method* to better approximate the full Hessian matrix. To further reduce the computational complexity per iteration, we directly compute the update step $(\Delta \mathbf{w})$ without computing and storing the full Hessian or its inverse. Furthermore, to address large-scale scenarios in which even computing a partial Hessian may require significant time, we used distribution-preserving (DP) sub-sampling to compute a partial Hessian. The DP sub-sampling generates p sub-samples with similar first and second-order distribution statistics and selects a single sub-sample at each epoch in a round-robin manner to compute the partial Hessian. We integrate our approximated Hessian with stochastic gradient descent and stochastic variance-reduced gradients to solve the logistic regression problem. The numerical experiments show that the proposed approach was able to obtain a better approximation of Newton's method with performance competitive with the state-of-the-art first-order and the stochastic quasi-Newton methods.

1 Introduction

The problem of the optimization of various function is among the most critical and popular topics in machine learning and mathematical optimization. Let $\{(\mathbf{x}_i, y_i)\}_{i=1}^n$ be given n training samples, where $\mathbf{x}_i \in \mathbb{R}^d$ and $y_i \in \{-1, 1\}$, and f be an objective function defined as follows.

$$\min_{\mathbf{w} \in \mathbb{R}^d} f(\mathbf{w}) = \frac{1}{n} \sum_{i=1}^n f_i(\mathbf{w}; \mathbf{x}_i, y_i) = \frac{1}{n} \sum_{i=1}^n f_i(\mathbf{w}), \quad (1)$$

where $f_i(\mathbf{w}; \mathbf{x}_i, y_i) : \mathbb{R}^d \rightarrow \mathbb{R}$ is the loss function. One of the well-known loss functions is a logistic regression $f_i(\mathbf{w}) = \log(1 + \exp(-y_i \mathbf{x}_i^T \mathbf{w}))$.

To optimize (1), first-order optimization methods such as stochastic gradient descent (SGD) [29], AdaGrad [13], stochastic variance-reduced gradient (SVRG) [20], SAGA [11], Adam [22], and the stochastic recursive gradient algorithm (SARAH), [28], possibly augmented with momentum, are preferred for large-scale optimization problems owing to their affordable computational costs, which are linear in dimensions per epoch $O(nd)$. However, the first-order methods are sensitive to hyperparameter choices and ineffective for ill-conditioned problems.

In contrast, Newton's method is independent of problem-dependent parameters and requires only minimal hyperparameter tuning for self-concordant functions such as ℓ_2 -regularized logistic regression. However, Newton's method

involves a computational complexity of $\Omega(nd^2 + d^{2.37})$ [1] per iteration, and thus is not suitable in large-scale settings. To reduce this computational complexity, the sub-sampled Newton method and random projection (or sketching) are commonly used by reducing the dimensions to solve the problem in a lower-dimensional subspace. Sub-sampled Newton method perform well for large-scale but relatively low dimensional problems by computing the Hessian matrix on a relatively smaller sample. However, the approximated Hessian can have a significant deviation from the full Hessian for high-dimensional problems. Randomized algorithms [24] estimate the Hessian in Newton's method through a random embedding matrix $\mathbf{S} \in \mathbb{R}^{m \times n}$ $\mathbf{H}_{\mathbf{S}}(\mathbf{w}) := (\nabla^2 f(\mathbf{w})^{\frac{1}{2}})^T \mathbf{S}^T \mathbf{S} \nabla^2 f(\mathbf{w})^{\frac{1}{2}}$. However, their approximation used $\nabla^2 f(\mathbf{w})^{\frac{1}{2}} = [\ell''(\mathbf{x}_1^T \mathbf{w})^{\frac{1}{2}} \mathbf{x}_1, \dots, \ell''(\mathbf{x}_n^T \mathbf{w})^{\frac{1}{2}} \mathbf{x}_n]^T$ as a low-rank approximation instead of deriving from actual curvature information while \mathbf{S} is a random projection matrix. Thus, the approximation may deviate significantly from the actual value. Other sketch matrix-based approximations to scale the Newton step computation were proposed with deterministic updates, and are therefore unsuitable for large-scale settings.

In contrast, the limited-memory Broyden-Fletcher-Goldfarb-Shanno (LBFGS) algorithm [26] is a widely used stochastic quasi-Newton method. However, it estimates the Hessian inverse using the past difference of gradients and updates. The online BFGS (oBFGS) [30] method is a stochastic version of regularized BFGS and L-BFGS with gradient descent. [23] proposed two variants of a stochastic quasi-Newton method incorporating a variance-reduced gradient. The first variant used a sub-sampled Hessian with singular value thresholding, which is numerically weaker. The second variant used the LBFGS method to approximate the Hessian inverse. Because these quasi-Newton methods approximate the Hessian inverse using first-order gradients, they are often unable to provide significant curvature information. The stochastic quasi-Newton method (SQN) [7] used the Hessian vector product computed on a subset of each mini-batch instead of approximating the Hessian inverse from the difference between the current and previous gradients, as in LBFGS. In contrast, SVRG-SQN [27] also incorporated variance-reduced gradients. Hence, both SQN and SVRG-SQN perform well with low-dimensional datasets, whereas their computational time cost drastically increases for high-dimensional datasets.

Recently, [35] approximated the Hessian inverse \mathbf{B} by decomposing it into two parts such that $\mathbf{B} = \mathbf{B}_1 + \mathbf{B}_2$, where \mathbf{B}_1 is either a sub-sampled Hessian, generalized Gauss-Newton matrix, Fisher information matrix, or any other approximation and \mathbf{B}_2 is the L-BFGS approximation. Observe that using the subsample Hessian can efficiently compute \mathbf{B}_1 for low-dimensional problems. However, it is important to note that on high-dimensional data where d is significantly large, computing the subsample Hessian or Fisher information matrix \mathbf{B}_1 can be computationally expensive because it takes $O(nd^2)$ time and $O(d^2)$ memory. Additionally, computing the sub-sample Hessian or Fisher information matrix at each iteration makes it more computationally intensive.

In this study, we overcome the limitation of the quasi-Newton's method and further enhance the curvature information used to approximate the Newton step through k -rank approximation of the Hessian matrix. In contrast to quasi-Newton methods that estimate the curvature information using first-order gradients only, we used Nyström approximation on the partial Hessian matrix ($d \times m$) constructed for the $m \ll d$ randomly selected columns only to estimate the Hessian matrix. Thus, our approximation is also more suitable for high-dimensional cases. We used our approximation with stochastic gradient descent (SGD) and stochastic variance-reduced gradient methods (SVRG), and theoretically proved their convergence. In addition, we evaluated the performance of the proposed approach on several large-scale datasets with a wide range of dimensions. The experiments show that the proposed methods consistently performed better than or competitively with existing methods, whereas the behavior of existing methods change significantly with the problem.

2 Preliminaries

The foundation of our algorithm is based on the Nyström approximation [12] of symmetric positive semi-definite matrix, defined as

Definition 1 (Nyström approximation). *Let $\mathbf{H} \in \mathbb{R}^{d \times d}$ be a symmetric positive semi-definite matrix, then k rank ($k \ll d$)*

approximation N_k of matrix H is given by

$$\begin{aligned}
N_k &= CM_k^\dagger C^T \\
&= C(U_k \Sigma_k U_k^T)^\dagger C^T && (\text{using } k\text{-SVD}) \\
&= C(U_k \Sigma_k^{-1} U_k^T) C^T \\
&= (CU_k \Sigma_k^{-1/2})(CU_k \Sigma_k^{-1/2})^T \\
&= ZZ^T,
\end{aligned} \tag{2}$$

where $C \in \mathbb{R}^{d \times m}$ is a matrix consisting m columns ($m \ll d$) of M , and M_k^\dagger is the best k -rank approximation of M , which formed by the intersection between those k columns of H and the corresponding k rows of H , and M_k^\dagger is pseudo-inverse of M_k and rank of M is k . To obtain the pseudo-inverse, we first compute the SVD of M_k as $M_k = U \Sigma U^T$.

Theoretically, the k -SVD is the best k -rank approximation of a symmetric positive semi-definitive matrix, but it requires the full matrix beforehand, whereas Nyström approximation can be used with the partial matrix. Theorem 1 gives the error bound for the Nyström approximation with respect to the best k -rank approximation.

Theorem 1. Let H be a $d \times d$ matrix and H_k be the best k -rank approximation of the H . Then, for $O(k/\epsilon^4)$ columns

$$\|H - CM_k^\dagger C^T\|_\nu \leq \|H - H_k\|_\nu + \epsilon \sum_{i=1}^d H_{ii}^2, \tag{3}$$

where $\epsilon > 0$ and $\nu = 2, F$ for spectral and Frobenius norms, respectively.

For the proof of Theorem 1 refer [12, Proof of Theorem 3].

To compute the inverse of the sum of an invertible matrix A and the outer product, UV^T , of U and V , we used the Sherman-Morrison-Woodbury formula, defined as given below.

Definition 2 (Sherman-Morrison-Woodbury). Let $A \in \mathbb{R}^{d \times d}$ matrix and $U, V \in \mathbb{R}^{d \times k}$. Then, the inverse of $(A + UV^T)$ is defined as

$$(A + UV^T)^{-1} = A^{-1} - A^{-1}U(I_k + V^T A^{-1}U)^{-1}V^T A^{-1}. \tag{4}$$

3 Proposed method

In this section, we propose Nyström stochastic gradient descent (NSGD) and stochastic variance-reduced gradient (NSVRG) methods.

3.1 Nyström SGD and SVRG methods

In the proposed method, to incorporate a better approximation of the curvature information, we use a low-rank approximation of the Hessian matrix. Because the Hessian matrix of a binary logistic regression is positive semi-definite, the Nyström approximation can be applied to obtain the low-rank approximation of the Hessian. At each epoch, we uniformly sample m columns as $\Omega \subset \{1, \dots, d\}$, where $m \ll d$, unlike all columns, as in [36]. Then, we compute a partial Hessian matrix $C \in \mathbb{R}^{d \times m}$ as the Jacobian of $\nabla f(w)$ with respect to w_Ω . This calculation requires $O(ndm)$ computational time. Then, by using Nyström method in (2), the k -rank approximate Hessian can be computed as

$$N_k = ZZ^T. \tag{5}$$

We compute $N_{k,\tau}$ at each epoch τ . For simplicity, we drop the subscript k and use N_τ to represent the k -rank approximation of the Hessian at epoch τ . Now, we use the regularized Nyström to ensure non-singularity by introducing the regularized parameter $\rho > 0$ by making the computation ρ -regularized. That is, $(N_\tau + \rho I)$ is positive definite. Therefore, $B_\tau = (N_\tau + \rho I)^{-1}$ generates good descent directions. Then, we update the iteration as

$$\mathbf{w}_t = \mathbf{w}_{t-1} - \eta B_\tau \mathbf{v}_{t-1}, \quad (6)$$

where \mathbf{v}_t denotes the appropriate stochastic gradient. *i.e.*, SGD or SVRG, etc. The proposed method for approximating the Hessian is shown in Figure 1, and computing the approximate Newton step with stochastic reduced variance in Algorithm 1 and with stochastic gradient is presented in Algorithm 2.

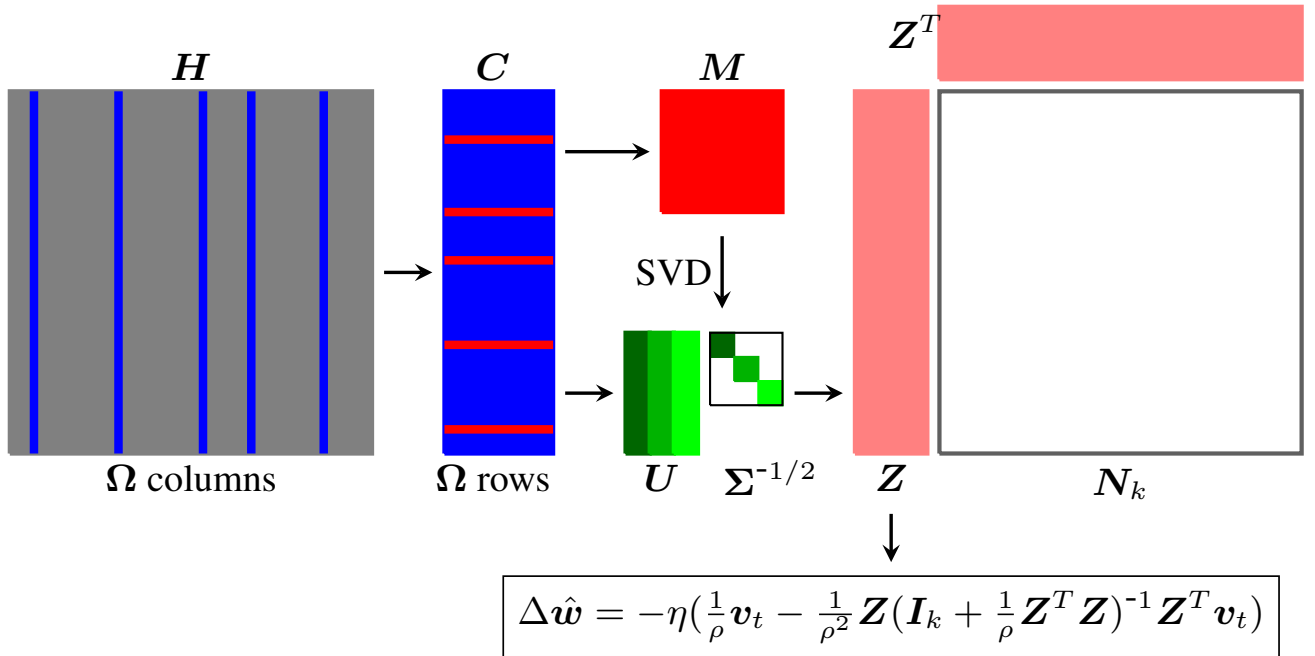


Figure 1: Computation of the $\Delta \mathbf{w}$ using Nyström-approximated Hessian.

3.2 Memory-efficient variant of NSGD and NSVRG

Storage and computation of the inverse of $(N_\tau + \rho I)$ requires $O(d^2)$ memory and $O(d^3)$ time. Thus, the simple implementation of NSGD and NSVRG may not be suitable for high-dimensional data. To reduce these computational requirements, we compute $B_\tau \mathbf{v}_{t-1}$ in (6) as

$$B_\tau \mathbf{v}_{t-1} = (N_\tau + \rho I)^{-1} \mathbf{v}_{t-1} = (\mathbf{Z}_\tau \mathbf{Z}_\tau^T + \rho I)^{-1} \mathbf{v}_{t-1}. \quad (7)$$

Then, we use (4) to further simplify the (7) as

$$\begin{aligned} B_\tau \mathbf{v}_{t-1} &= \frac{1}{\rho} \mathbf{v}_{t-1} - \frac{1}{\rho^2} \mathbf{Z}_\tau (\mathbf{I}_k + \frac{1}{\rho} \mathbf{Z}_\tau^T \mathbf{Z}_\tau)^{-1} \mathbf{Z}_\tau^T \mathbf{v}_{t-1} \\ &= \frac{1}{\rho} \mathbf{v}_{t-1} - \mathbf{Q}_\tau \mathbf{Z}_\tau^T \mathbf{v}_{t-1}, \end{aligned} \quad (8)$$

Algorithm 1 Nyström SVRG Algorithm

Parameters: Update frequency ℓ and initial step size η_0

```
1: Initialize  $\tilde{w}_0$ 
2: for  $\tau = 1, 2, \dots$  do
3:    $\tilde{w} = \tilde{w}_{\tau-1}$ 
4:    $\tilde{g} = \frac{1}{n} \sum_{i=1}^n \nabla f_i(\tilde{w})$ 
5:    $\mathcal{S} = \begin{cases} \{1, \dots, n\} & \text{for NSVRG,} \\ \mathcal{S}_p, p = \tau \pmod{P} & \text{for NSVRG-D} \end{cases}$ 
6:    $C = \frac{\partial \nabla f_{\mathcal{S}}(\tilde{w})}{\partial \tilde{w}_{\Omega}}$ , where  $\Omega \subset \{1, \dots, d\}, |\Omega| = m$ 
7:   compute  $Z_{\tau}$  using (2)
8:    $Q_{\tau} = \frac{1}{\rho^2} Z_{\tau} (I_k + \frac{1}{\rho} Z_{\tau}^T Z_{\tau})^{-1}$ 
9:    $w_0 = \tilde{w}$ 
10:  for  $t = 1, \dots, \ell$  do
11:    randomly pick batch  $\mathcal{B} \sim \{1, \dots, n\}$ 
12:     $v_{t-1} = \nabla f_{\mathcal{B}}(w_{t-1}) - \nabla f_{\mathcal{B}}(\tilde{w}) + \tilde{g}$ 
13:    Compute  $B_{\tau} v_{t-1}$  using (8)
14:     $w_t = w_{t-1} - \eta B_{\tau} v_{t-1}$ 
15:  end for
16:   $\tilde{w}_{\tau} = w_t$  for randomly chosen  $t \in \{1, \dots, \ell\}$ 
17: end for
```

Algorithm 2 Nyström SGD Algorithm

Parameters: Update frequency ℓ and initial step size $\eta_0 = \beta$

```
1: Initialize  $w_0, \tau = 1$ 
2: for  $t = 1, 2, \dots$  do
3:   randomly pick batch  $\mathcal{B} \sim \{1, \dots, n\}$ 
4:    $v_{t-1} = \nabla f_{\mathcal{B}}(w_{t-1})$ 
5:   if  $(t-1) \bmod \ell = 0$  then
6:      $\mathcal{S} = \begin{cases} \{1, \dots, n\} & \text{for NSGD,} \\ \mathcal{S}_p, p = \tau \pmod{P} & \text{for NSGD-D} \end{cases}$ 
7:      $C = \frac{\partial \nabla f_{\mathcal{S}}(w)}{\partial w_{\Omega}}$ , where  $\Omega \subset \{1, \dots, d\}, |\Omega| = m$ 
8:     compute  $Z_{\tau}$  using (2)
9:      $Q_{\tau} = \frac{1}{\rho^2} Z_{\tau} (I_k + \frac{1}{\rho} Z_{\tau}^T Z_{\tau})^{-1}$ 
10:     $\tau = \tau + 1$ 
11:   end if
12:   Compute  $B_{\tau-1} v_{t-1}$  using (8)
13:    $w_t = w_{t-1} - \eta B_{\tau-1} v_{t-1}$ 
14: end for
```

where $Q_{\tau} = \frac{1}{\rho^2} Z_{\tau} (I_k + \frac{1}{\rho} Z_{\tau}^T Z_{\tau})^{-1}$.

Thus far, the major computation $O(ndm)$ is taken for the computation of C . Note that $(I + \frac{1}{\rho} Z_{\tau} Z_{\tau}^T) \in \mathbb{R}^{k \times k}$, and its inverse can be computed much faster than the inverse of $(N_{\tau} + \rho I)$ directly. Because n becomes the most dominant under

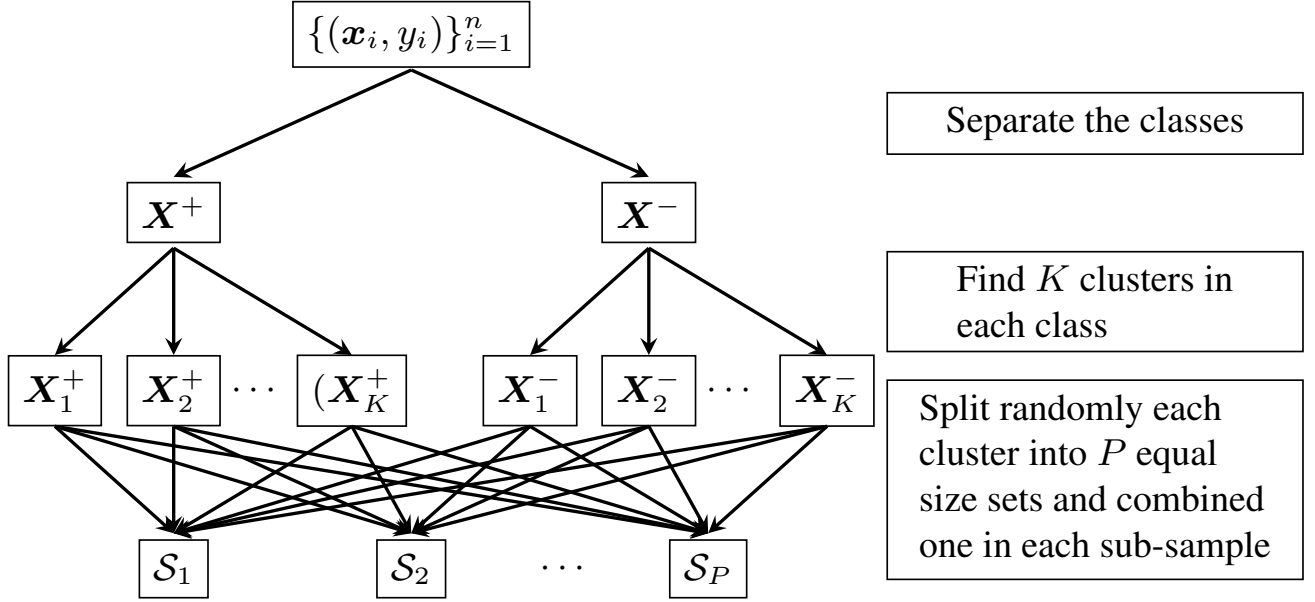


Figure 2: Distribution-Preserving Sub-sampling generation process. (The *pseudo-code* is in Appendix-C)

the large-scale settings in the computation of \mathbf{C} , we propose to compute the matrix \mathbf{C} on a sub-sample \mathcal{S} selected using DP sub-sampling similarly to [33], while the stochastic gradients were computed on the randomly selected mini-batches $\mathcal{B} \subset \{1, \dots, n\}$, thereby reducing the final computational cost of \mathbf{C} to $O(|\mathcal{S}|dm)$ or $O(ndm/P)$. We refer to these memory-efficient variants of NSGD and NSVRG as NSGD-D and NSVRG-D, respectively.

Distribution-Preserving Sub-sampling: The distribution-preserving (DP) sub-sampling first separates the classes to maintain the same class ratio as in the full dataset. Then, each class is grouped into K clusters using the kmeans algorithm. The clusters generated by kmeans have the least variability in a cluster, while having high variability across clusters. Because the data points in each generated cluster have the least variance, splitting them uniformly into P sub-samples would not cause a significant deviation of its statistical properties. The process of DP sub-sampling is presented in Figure 2. Finally, each sub-sample generated using DP sub-sampling has an equal number of samples from all clusters of each class, preserving the class ratio and first-and second-order statistical properties of the entire data in each generated sub-sample.

3.3 Computational Complexity

Here, we analyze the per-epoch computational complexity of the proposed method. First, it is important to note that $\mathbf{Z}_\tau, \mathbf{Q}_\tau \in \mathbb{R}^{d \times k}$ is computed at each epoch, whereas (8) is computed at each iteration. The cost of matrix-vector multiplication $\mathbf{B}_\tau \mathbf{v}_t$, i.e., (8) is $O(dk)$ at each iteration, and therefore $O(\ell dk)$ per epoch, where ℓ denotes the iterations per epoch. The cost of computing \mathbf{Q}_τ is $O(dk^2)$ at each epoch. The cost of computing \mathbf{Z}_τ is $O(dmk)$. The computational cost to construct matrix \mathbf{C} is $O(ndm)$. Thus, in the entire epoch construction of the matrix \mathbf{C} is associated with the highest computational cost; therefore, the overall time and space complexity are $O(ndm)$ and $O(dm)$, respectively. However, it is important to note that the use of DP subsampling reduces the final computational cost of \mathbf{C} to $O(|\mathcal{S}|dk)$.

3.4 Convergence analysis

We show that the proposed method has suitable properties in both the computation and memory space. In this section, we present a convergence analysis, which involves the following assumptions.

Table 1: Per iteration space and time complexities.

Method	Time	Space
Newton	$O(nd^2 + d^3)$	$O(d^2)$
NSGD/NSVRG	$O(ndm)$	$O(dm)$
NSGD-D/NSVRG-D	$O(ndm/P)$	$O(dm)$

Assumption 1. We assume that each f_i is convex and twice continuously differentiable.

Assumption 2. There exists two positive constants μ and Λ such that

$$\mu \mathbf{I} \preceq \nabla^2 f_S(\mathbf{w}) \preceq \Lambda \mathbf{I}, \quad \mathbf{w} \in \mathbb{R}^d,$$

for a set $S \subseteq \{1, 2, \dots, n\}$. Note that the lower bound always holds in the regularized case.

Assumption 3. We assume that the gradient of each f_i is Λ -Lipschitz continuous, i.e.,

$$\|\nabla f_i(\mathbf{w}_a) - \nabla f_i(\mathbf{w}_b)\| \leq \Lambda \|\mathbf{w}_a - \mathbf{w}_b\| \quad \forall \mathbf{w}_a, \mathbf{w}_b \in \mathbb{R}^d.$$

Under this assumption, it is clear that ∇f is also Λ -Lipschitz continuous.

$$\|\nabla f(\mathbf{w}_a) - \nabla f(\mathbf{w}_b)\| \leq \Lambda \|\mathbf{w}_a - \mathbf{w}_b\| \quad \forall \mathbf{w}_a, \mathbf{w}_b \in \mathbb{R}^d.$$

Assumption 4. For a set $S \subseteq \{1, 2, \dots, n\}$, there exists two constants $0 \leq \gamma < \Gamma$ such that the Nyström approximation $\mathbf{Z}_S \mathbf{Z}_S^T$ of the original Hessian \mathbf{H}_S satisfies the following.

$$\gamma \mathbf{I} \preceq \mathbf{N}_S = \mathbf{Z}_S \mathbf{Z}_S^T \preceq \Gamma \mathbf{I}, \quad \mathbf{w} \in \mathbb{R}^d. \quad (9)$$

Next, we provide the bound of the regularized Nyström approximation $(\mathbf{N}_S + \rho \mathbf{I})$, with the help of the above assumption.

Lemma 1. Let Assumption 4 hold. Then, for set $S \subseteq \{1, \dots, n\}$, the following bounds exist.

$$(\gamma + \rho) \mathbf{I} \preceq (\mathbf{N}_S + \rho \mathbf{I}) \preceq (\Gamma + \rho \mathbf{I}), \quad \text{for } \rho > 0.$$

The following Lemma gives the bounds to the inverse approximation $\mathbf{B} = (\mathbf{N} + \rho \mathbf{I})^{-1}$ using the above Lemma.

Lemma 2. Let Assumption 1, 2 and 4 Hold. Then, the a set $S \subseteq \{1, \dots, n\}$ - regularized Nyström approximation $(\mathbf{N}_S + \rho \mathbf{I})^{-1}$ is bounded.

The following Lemma gives the upper bound of the variance of the variance-reduced gradient.

Lemma 3. Let \mathbf{w}_* be a unique minimizer of f and $\mathbf{v}_t = \nabla f_{\mathcal{B}}(\mathbf{w}_t) - \nabla f_{\mathcal{B}}(\tilde{\mathbf{w}}) + \nabla f(\tilde{\mathbf{w}})$ be a variance-reduced stochastic gradient with mini batch $\mathcal{B} \subseteq \{1, \dots, n\}$. Then, the expectation with respect to \mathcal{B} is bounded;

$$\mathbb{E} \|\mathbf{v}_t\|^2 \leq 4\Lambda(f(\mathbf{w}_t) - f(\mathbf{w}_*) + f(\mathbf{w}_\tau) - f(\mathbf{w}_*)).$$

This bound follows from the [27, Lemma 6] which closely follows from [20, Theorem 1].

At this point, we make use of Lemma 4, which states a result of a strongly convex function.

Lemma 4. Suppose that f is continuously differentiable and strongly convex with parameter μ . Let \mathbf{w}_* be a unique minimizer of f . Then, for any $\mathbf{w} \in \mathbb{R}$, we have

$$\|\nabla f(\mathbf{w})\|^2 \geq 2\mu(f(\mathbf{w}) - f(\mathbf{w}_*))$$

The next theorem states the main result for the convergence of Algorithm 1. We follow a similar analysis to that of [27].

Theorem 2. *Suppose Assumptions 1 - 4 hold, and let \mathbf{w}_* be a unique minimizer of the objective function (1). Then, for all $\tau \geq 0$,*

$$\mathbb{E}[f(\mathbf{w}_\tau) - f(\mathbf{w}_*)] \leq \alpha^\tau \mathbb{E}[f(\mathbf{w}_0) - f(\mathbf{w}_*)], \quad (10)$$

where

$$\alpha = \frac{1 + 2\ell\eta^2\Lambda^2\delta^2}{2\ell\eta(\mu\Delta - \eta\Lambda^2\delta^2)} < 1,$$

$\Delta = 1/(\Gamma + \rho)$, and $\delta = 1/(\gamma + \rho)$, assuming $\eta < \mu\Delta/2\Lambda^2\delta^2$ and choosing a sufficiently large ℓ to satisfy

$$\frac{1}{2\ell\eta} + 2\eta\Lambda^2\delta^2 < \mu\Delta. \quad (11)$$

Assumption 5. *There exists a constant θ such that for all $\mathbf{w} \in \mathbb{R}^d$,*

$$\mathbb{E}[\|\nabla f(\mathbf{w})\|^2] \leq \theta^2.$$

For Algorithm 2, we use the step size (learning rate) $\eta = \beta/t$ for $\beta > 0$, and follow an analysis similar to [7]. We consider the Newton-like iteration

$$\mathbf{w}_\tau = \mathbf{w}_{t-1} - \eta \mathbf{B}_\tau \nabla f(\mathbf{w}_{t-1}). \quad (12)$$

Note that Algorithm 2 is a special case of (12), where \mathbf{B}_τ , is constant for ℓ iterations.

Theorem 3. *Suppose Assumptions 1 - 5 holds. Let \mathbf{w}_τ be the iterates generated by the Newton-like method (12), where for $t = 1, 2, \dots$*

$$\Delta \mathbf{I} \preceq \mathbf{B}_\tau \preceq \delta \mathbf{I}.$$

$\eta = \beta/t$, and $\beta > 1/2\mu\Delta$, Then, for $t \geq 1$,

$$\mathbb{E}[f(\mathbf{w}_t) - f(\mathbf{w}_*)] \leq g(\beta)/t, \quad (13)$$

where

$$g(\beta) = \max \left\{ \frac{\beta^2 \Lambda \theta^2 \delta^2}{2(2\beta\mu\Delta - 1)}, f(\mathbf{w}_1) - f(\mathbf{w}_*) \right\}, \quad (14)$$

$\delta = 1/(\gamma + \rho)$, and $\Delta = 1/(\Gamma + \rho)$.

The following corollary establishes the convergence of Algorithm 2.

Corollary 1. *Suppose Assumptions 1 - 5 holds. Let \mathbf{w}_t be the iterates generated by Algorithm 2. Then, there exist two positive constants Δ such that $\|\mathbf{B}_\tau^{-1}\| \leq 1/\Delta$, and if $\eta = \beta/t$ where $\beta > 1/2\mu\delta$, Then, for all $\tau \geq 1$,*

$$\mathbb{E}[f(\mathbf{w}_t) - f(\mathbf{w}_*)] \leq g(\beta)/t, \quad (15)$$

where $\delta = 1/(\gamma + \rho)$, $\Delta = 1/(\Gamma + \rho)$, and

$$g(\beta) = \max \left\{ \frac{\beta^2 \Lambda \theta^2 \delta^2}{2(2\beta\mu\Delta - 1)}, f(\mathbf{w}_1) - f(\mathbf{w}_*) \right\}.$$

Proofs are provided in Appendix A for all of the above Lemmas and Theorems, as well as the Corollary.

4 Related work

The evolution of approximations of the Hessian or its inverse begins with the DFP [10, 15], Broyden [5], SR1 [8], and well-known BFGS methods [6, 14, 16, 32]. The BFGS method uses secant equations to approximate the Hessian inverse and requires $O(d^2)$ memory to store the approximate Hessian. Recently, [26] proposed a limited-memory BFGS (L-BFGS) to solve the large-scale unconstrained optimization problem. They used L-BFGS to compute an approximation of the Hessian inverse using $O(md)$ memory instead of $O(d^2)$, where $m \ll d$.

To address the increased demand for optimization in machine learning and deep learning, various first-order stochastic optimization methods [20, 13, 11, 22, 28] have been proposed, but their sensitivity to the choice of hyperparameters remains a concern. Owing to the low sensitivity of the choice of hyperparameters, stochastic quasi-Newton methods have gained popularity in recent years. A stochastic quasi-Newton method by [7] proposed an approximated sub-sampled Hessian using the Hessian vector product instead of using the difference of gradients in the secant equation. [27] proposed a stochastic L-BFGS using a similar technique along with mini-batch variance-reduced gradients. [23] proposed a strategy to compute the sub-sample Hessian followed by the singular value thresholding. As a generalization of quasi-Newton methods, [31] proposed the use of robust symmetric multi-secant updates to approximate the Hessian. [2] reduced the amount of computation required to compute the gradient difference in the secant equation by using overlapping batches instead of computing them twice.

Building on these methods, [4] proposed progressive batching. [35] computed computationally inexpensive and expensive part of the Hessian using low-rank and L-BFGS approximation, respectively. Recently, a few works have investigated the Kronecker-factored-based second-order approximations. [18] proposed Kronecker-factored approximate curvature. [17] proposed a practical quasi-Newton called K-BFGS. Moreover, [34] explored a distributed quasi-Newton method and demonstrated its good theoretical properties.

5 Numerical Experiments

We evaluated the performance of the proposed methods on the several benchmark datasets given in Table 2.

Table 2: Details of the datasets used in the experiments

Dataset	Dim	Train	Test
<i>adult</i> [*]	123	32,561	16,281
<i>w8a</i> [*]	300	49,749	14,951
<i>mnist</i> [†]	784	60,000	10,000
<i>cifar10</i> [‡]	3,072	50,000	10,000
<i>real-sim</i> [*]	20,958	57,909	14,400

5.1 Baseline methods

We compared the proposed methods with the existing *state-of-the-art* first and second order optimization methods, namely, SGD, SVRG, Adam, S4QN [35], SVRG-LBFGS [23], oBFGS [30], SVRG-SQN [27], and SQN [7]. We compare various variants of the proposed methods, namely, Nyström SVRG (NSVRG), Nyström SVRG with DP sub-sampling (NSVRG-D), Nyström SGD (NSGD), and Nyström SGD with DP sub-sampling (NSGD-D) for optimization error and classification accuracy on both training and test data.

^{*}Available at LIBSVM [9] <https://www.csie.ntu.edu.tw/~cjlin/libsvm/>

[†]The original 10 classes in the MNIST are converted to the binary classes based on the round (0,3,6,8,9) vs. non-round (1,2,4,5,7) digits, similar to [25, 37]

[‡]The original 10 classes in the CIFAR10 are converted to the binary classes based on the natural (bird, cat, deer, dog, frog, horse) vs. man-made (airplane, automobile, ship, truck) objects, similar to [19]

5.2 Experimental Setup

We demonstrate the performance of the proposed and existing methods on the ℓ_2 -regularized logistic regression problem with the regularizer $\lambda \in \{10^{-2}, 10^{-3}, 10^{-4}\}$. For each λ , all methods were tuned for other hyperparameters such as $\eta \in \{10^0, 10^{-1}, 10^{-2}, 10^{-3}, 10^{-4}, 10^{-5}\}$, batch size, epochs, etc. The parameter $m = 50$ and $\rho \in \{10^3, 10^2, 10^1, 10^0, 10^{-1}, 10^{-2}, 10^{-3}, \|\mathbf{Z}\|_F\}$ were specific to the proposed variants only. In the DPP sampling, we set the number of clusters $K = 50$, the number of partitions $P = 10$, and the maximum number of iterations for the k -means algorithm was set to 10. The memory used in the quasi-Newton method was set to 20, which is a commonly used value [23, 7]. We chose an initial point very close to the optimal solution to eliminate the possibility of an exceptionally large initial error. The closed-form solution of the least-squares problem was initialized as the solution. Let $(\mathbf{A}, \mathbf{b}) \subseteq (\mathbf{X}, \mathbf{y})$ be a subsample from the training dataset; then, the initial point $\mathbf{w}_0 = (\mathbf{A}^T \mathbf{A} + \lambda \mathbf{I})^{-1} \mathbf{A}^T \mathbf{b}$. We report the optimization error on the training set (Opt. Error) and testing set (test error) with respect to epochs and training CPU time cost per epoch. The best-performing model was selected based on the minimum optimization error on the training set and presented its corresponding validation error. We implemented the existing and proposed methods in MATLAB using the SGDLibrary [21]. We computed the results shown in Figure 3 on an Intel(R) Xeon(R) CPU E5-2690v4 @ 2.60GHz with 14 cores and all other results on an Intel(R) Xeon(R) CPU E5-2698v4 @ 2.20GHz with 40 cores running MATLAB R2019a.

5.3 Results

To show the quality of the approximate curvature information used in the proposed methods, we present a comparison of the proposed methods with first-order methods (SGD and SVRG) used as the base for our algorithms in Figure 3 on *w8a* and *adult* datasets. The difference between SGD and NSGD-D (similarly SVRG and NSVRG-D) on both datasets clearly shows the benefits of using the approximate curvature information and the quality of the approximation. methods, Figure 3 also presents a performance comparison with the recently proposed state-of-the-art S4QN method [35]. For S4QN, we used two variants with sub-sampled Newton (S4QN-N) and Fisher information matrix (S4QN-F) as the base matrix and set $r_1 = 0.1$ and $r_2 = 10$. Because sub-sampled Hessian and FIM were the same for the logistic regression, both resulted in a similar optimization. However, S4QN-F was relatively faster than S4QN-N because of the low computational cost of FIM. The time taken in the initial epoch by S4QN is significantly higher, as it computes Hessian on a sub-sample at each update. However, the use of a growing gradient batch size reduces the frequency of updates per epoch to speed up subsequent epochs, but decreases the quality of curvature information. Hence, no significant improvement may be observed in the optimization error. However, the proposed NSGD-D and NSVRG-D outperformed both variants of the S4QN, indicating that the proposed methods use a better approximation of the curvature information.

Figure 4, 5, and 6 show the comparisons of the proposed methods with Adam and existing quasi-Newton methods. We present the numerical results per epoch as well as per epoch in terms of CPU time. It may be observed from the results that the proposed methods performed better than or very competitively with the existing methods consistently on all the datasets with the varying number of dimensions and samples. Additionally, the performance of the proposed methods was almost stable when increasing the regularization parameters, whereas that of the existing methods changed significantly. The existing methods such as SVRG-LBFGS and OBFSGS sometimes performed very competitively to the proposed methods. However, their performance was not very stable as they could fluctuate significantly even after reaching very close to the optimal point. Also, a consistently low validation error on all datasets illustrated the generalization ability of the trained model compared to existing methods.

It may be observed from the results that the proposed methods generated robust curvature information using only 50 columns of Hessian in the Nyström approximation, compared to the existing quasi-Newton methods using traditional secant equation. It is also important to note that NSVRG-D and NSGD-D exhibited similar behavior to NSVRG and NSGD, respectively. Moreover, both DP sub-sampling variants required less CPU time compared to NSVRG and NSGD. As we took the initial point \mathbf{w}_0 to be the solution of the least squares problem, the first-order method Adam was unable to significantly reduce the optimization cost. It may be observed that existing stochastic methods require long CPU times for problems with higher dimensionality. More precisely, for the *cifar* dataset, OBFSGS and SQN required more time to reach the optimal point.

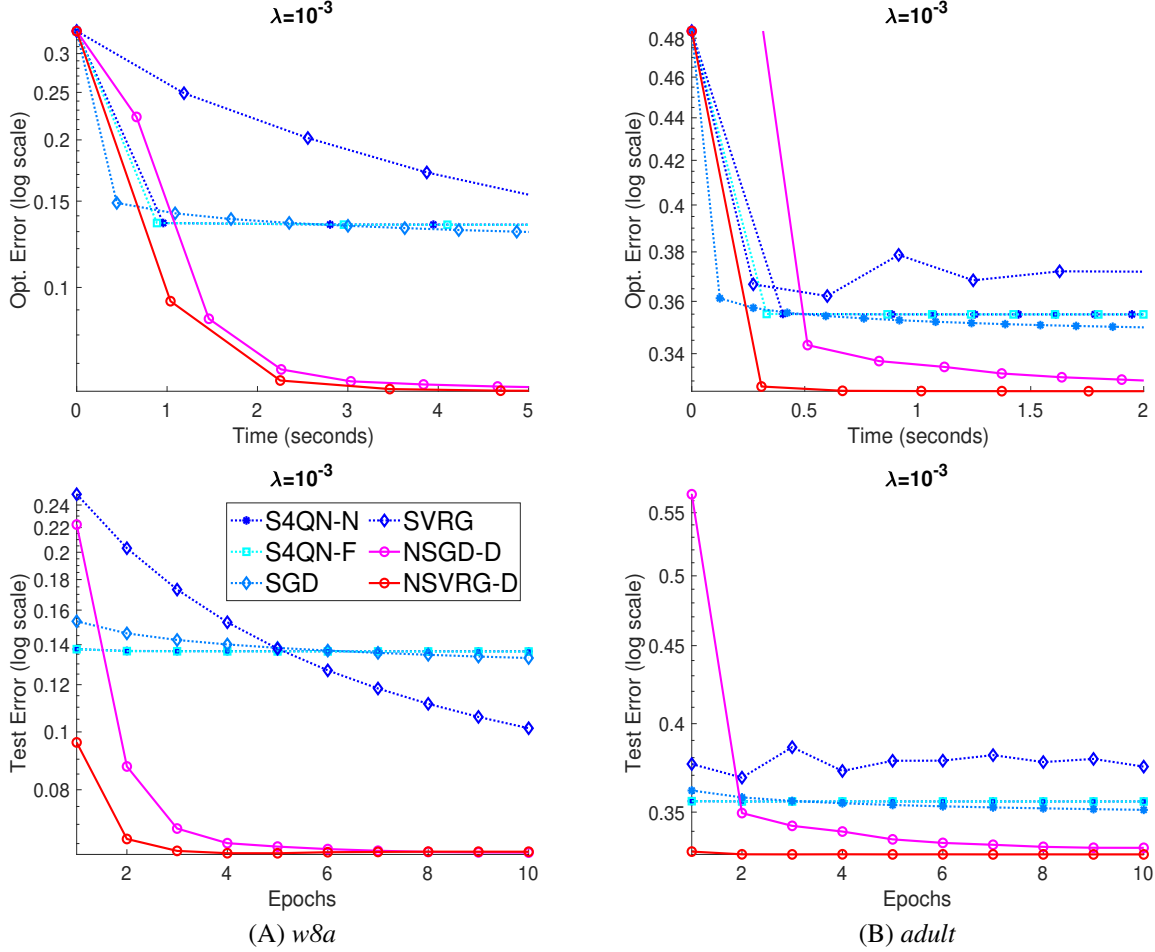


Figure 3: Comparison of proposed methods with S4QN, SGD, and SVRG on *w8a* and *adult* datasets.

In *mnist* and *real-sim* datasets, SQN and SVRG-SQN require a considerable period of time to reach the optimal point.

6 Conclusion

In terms of optimal cost, the proposed methods performed better than first-order methods, namely, Adam, SGD, and SVRG, and performed better than or comparably to stochastic quasi-Newton methods, namely, SVRG-LBFGS, oBFGS, SVRG-SQN, and SQN. In terms of computational time, our methods performed much better than Newton's method, while remaining competitive with stochastic quasi-Newton methods. Additionally, experimental results on several publicly available benchmark datasets show that the proposed method exhibited much more stable and generalized behavior in comparison to both first- and second-order methods, which can be attributed to the better preservation of the curvature information through Nyström approximation of the Hessian matrix. The proposed method can be applied to deep models; in particular, it would significantly reduce the computational time required for Hessian estimation for fully connected layers where the number of parameters is very large.

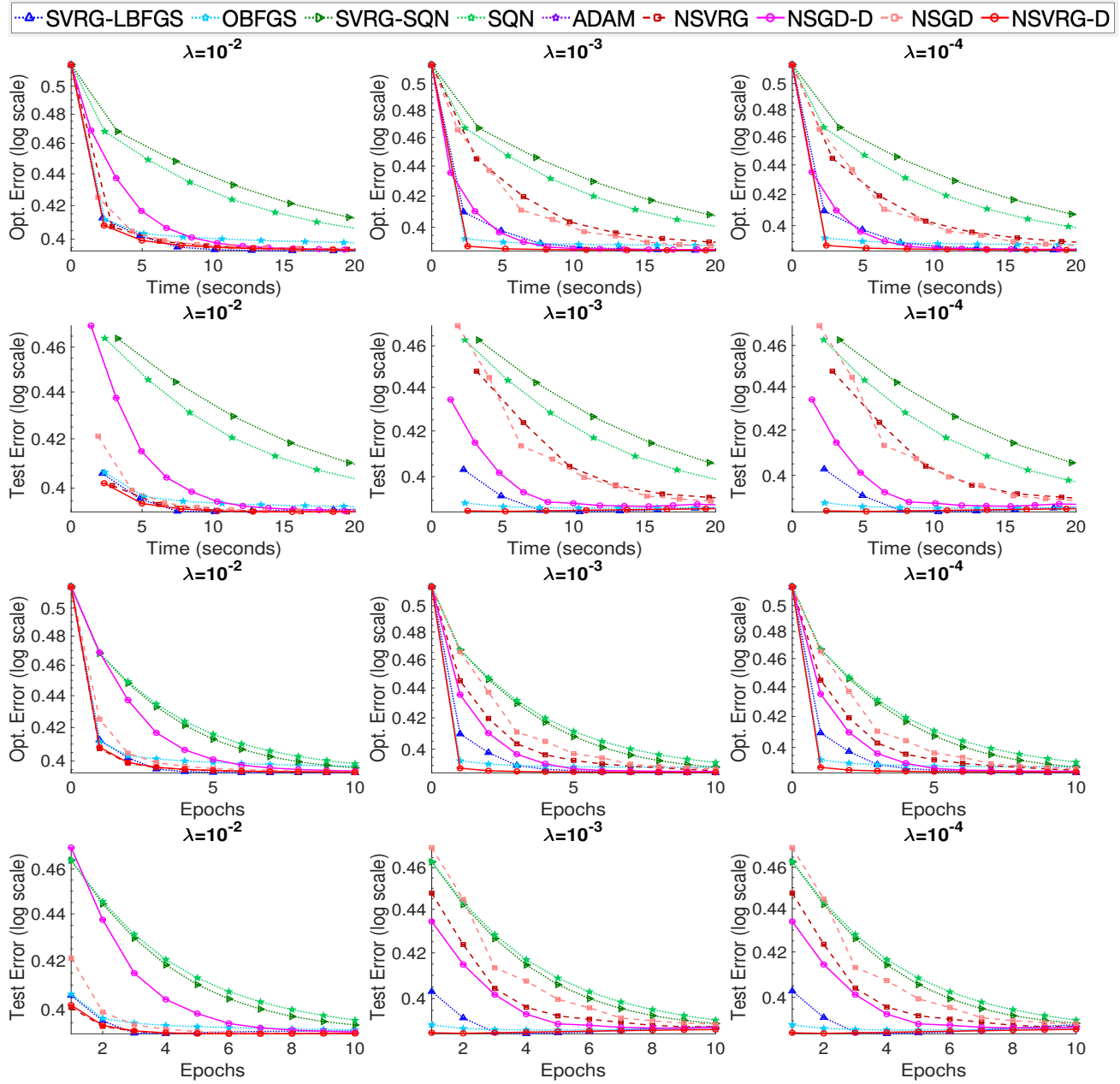


Figure 4: Comparison on *mnist* dataset.

References

- [1] Naman Agarwal, Brian Bullins, and Elad Hazan. Second-order stochastic optimization for machine learning in linear time. *Journal of Machine Learning Research, JMLR*, 18:116:1–116:40, 2017.

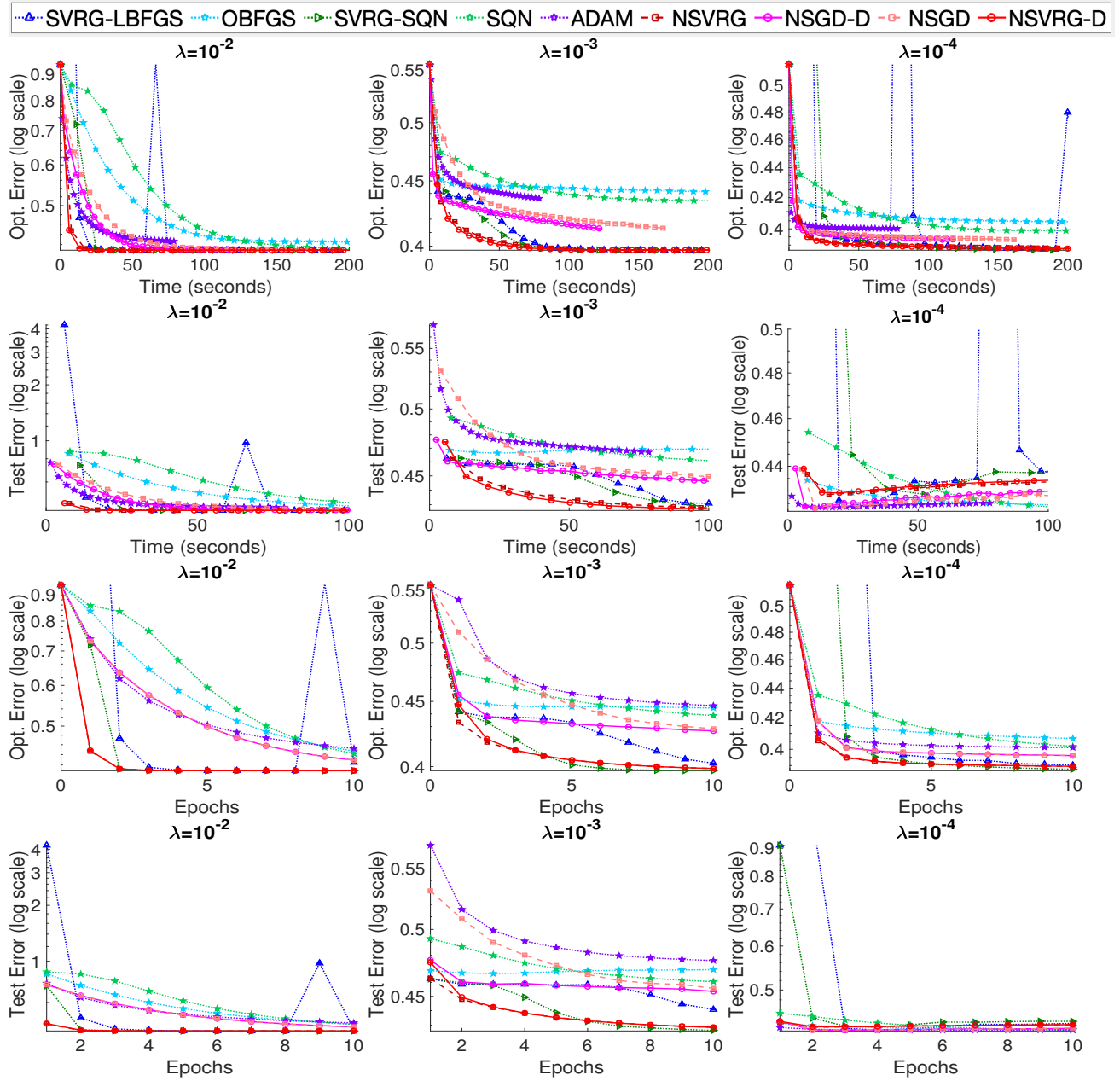


Figure 5: Comparison on *cifar10* dataset.

- [2] Albert S. Berahas, Jorge Nocedal, and Martin Takác. A multi-batch L-BFGS method for machine learning. In *Advances in Neural Information Processing Systems, NIPS*, pages 1055–1063, 2016.
- [3] Rajendra Bhatia. *Matrix Analysis*, volume 169. Springer Science & Business Media, 2013.
- [4] Raghu Bollapragada, Jorge Nocedal, Dheevatsa Mudigere, Hao-Jun Shi, and Ping Tak Peter Tang. A progressive

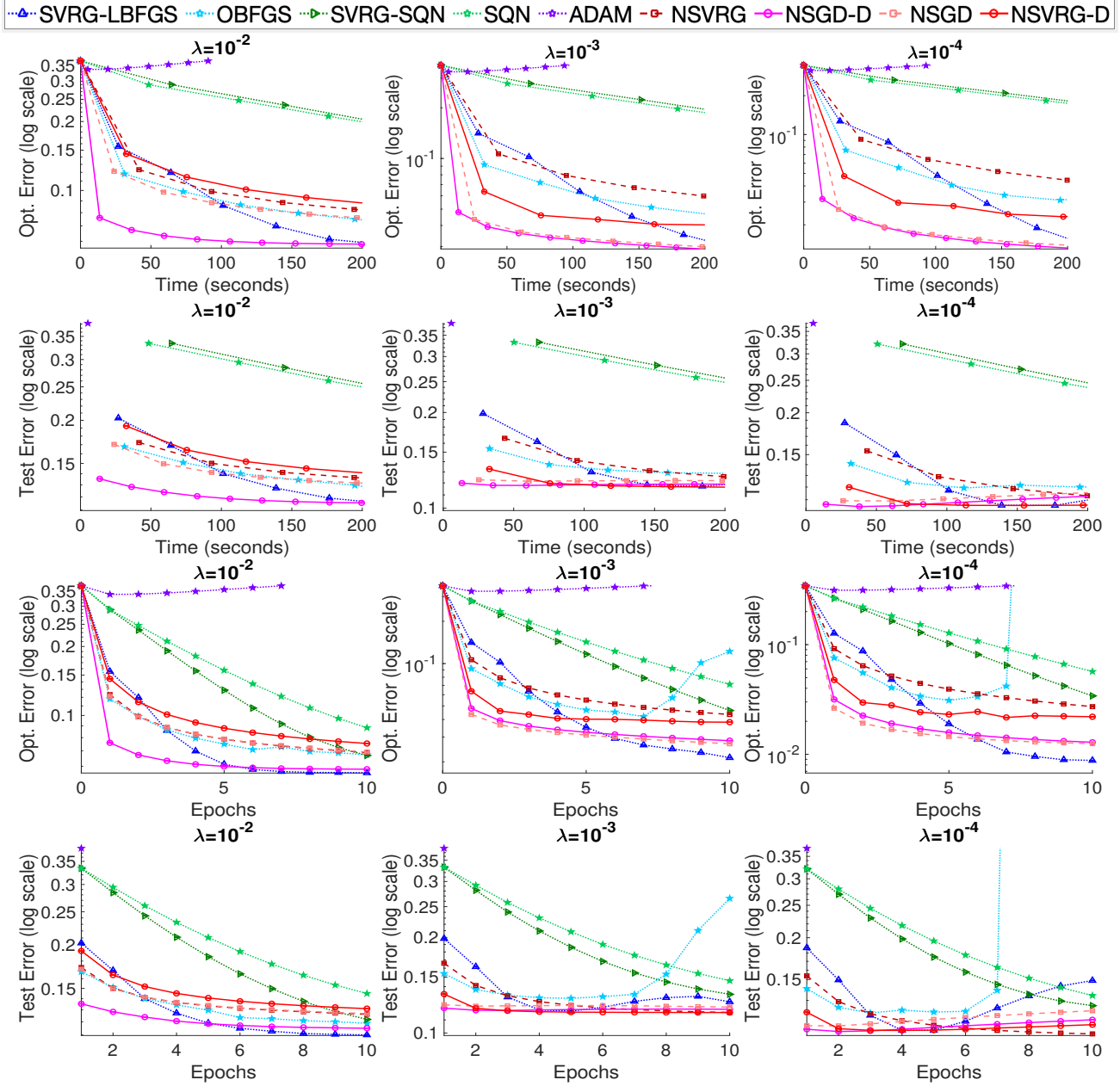


Figure 6: Comparison on *real-sim* dataset.

batching l-bfgs method for machine learning. In *Proceedings of the International Conference on Machine Learning, ICML*, pages 620–629, 2018.

- [5] Charles G Broyden. A class of methods for solving nonlinear simultaneous equations. *Mathematics of Computation*, 19(92):577–593, 1965.

- [6] Charles G Broyden. A new double-rank minimisation algorithm. preliminary report. In *Notices of the American Mathematical Society*, volume 16, page 670, 1969.
- [7] Richard H Byrd, Samantha L Hansen, Jorge Nocedal, and Yoram Singer. A stochastic quasi-newton method for large-scale optimization. *SIAM Journal on Optimization*, 26(2):1008–1031, 2016.
- [8] Richard H Byrd, Humaid Fayez Khalfan, and Robert B Schnabel. Analysis of a symmetric rank-one trust region method. *SIAM Journal on Optimization*, 6(4):1025–1039, 1996.
- [9] Chih-Chung Chang and Chih-Jen Lin. LIBSVM: A library for support vector machines. *ACM Transactions on Intelligent Systems and Technology*, 2:27:1–27:27, 2011.
- [10] W C Davidon. Variable metric method for minimization. 5 1959.
- [11] Aaron Defazio, Francis Bach, and Simon Lacoste-Julien. SAGA: A fast incremental gradient method with support for non-strongly convex composite objectives. In *Advances in Neural Information Processing Systems, NIPS*, pages 1646–1654, 2014.
- [12] Petros Drineas and Michael W. Mahoney. On the nyström method for approximating a gram matrix for improved kernel-based learning. *Journal of Machine Learning Research, JMLR*, 6:2153–2175, 2005.
- [13] John Duchi, Elad Hazan, and Yoram Singer. Adaptive subgradient methods for online learning and stochastic optimization. *Journal of Machine Learning Research, JMLR*, 12(7), 2011.
- [14] Roger Fletcher. A new approach to variable metric algorithms. *The Computer Journal*, 13(3):317–322, 1970.
- [15] Roger Fletcher and Michael JD Powell. A rapidly convergent descent method for minimization. *The Computer Journal*, 6(2):163–168, 1963.
- [16] Donald Goldfarb. A family of variable-metric methods derived by variational means. *Mathematics of Computation*, 24(109):23–26, 1970.
- [17] Donald Goldfarb, Yi Ren, and Achraf Bahamou. Practical quasi-newton methods for training deep neural networks. In *Advances in Neural Information Processing Systems, NIPS*, pages 2386–2396, 2020.
- [18] Roger B. Grosse and James Martens. A kronecker-factored approximate fisher matrix for convolution layers. In *Proceedings of the International Conference on Machine Learning, ICML*, pages 573–582, 2016.
- [19] Cho-Jui Hsieh, Si Si, and Inderjit S. Dhillon. A divide-and-conquer solver for kernel support vector machines. In *Proceedings of the International Conference on Machine Learning, ICML*, pages 566–574, 2014.
- [20] Rie Johnson and Tong Zhang. Accelerating stochastic gradient descent using predictive variance reduction. In *Advances in Neural Information Processing Systems, NIPS*, pages 315–323, 2013.
- [21] Hiroyuki Kasai. Sgdl library: A MATLAB library for stochastic optimization algorithms. *Journal of Machine Learning Research, JMLR*, 18:215:1–215:5, 2017.
- [22] Diederik P. Kingma and Jimmy Ba. Adam: A method for stochastic optimization. In Yoshua Bengio and Yann LeCun, editors, *Proceedings of the International Conference on Learning Representations, ICLR*, 2015.
- [23] Ritesh Kolte, Murat Erdogdu, and Ayfer Ozgur. Accelerating svrg via second-order information. In *NIPS Workshop on Optimization for Machine Learning*, 2015.

- [24] Jonathan Lacotte, Yifei Wang, and Mert Pilanci. Adaptive newton sketch: Linear-time optimization with quadratic convergence and effective hessian dimensionality. In Marina Meila and Tong Zhang, editors, *Proceedings of the 38th International Conference on Machine Learning, ICML*, volume 139, pages 5926–5936, 2021.
- [25] Liang Lan, Zhuang Wang, Shandian Zhe, Wei Cheng, Jun Wang, and Kai Zhang. Scaling up kernel SVM on limited resources: A low-rank linearization approach. *IEEE Transactions on Neural Networks and Learning Systems, TNNLS*, 30(2):369–378, 2019.
- [26] Dong C Liu and Jorge Nocedal. On the limited memory bfgs method for large scale optimization. *Mathematical Programming*, 45(1):503–528, 1989.
- [27] Philipp Moritz, Robert Nishihara, and Michael Jordan. A linearly-convergent stochastic l-bfgs algorithm. In *Proceedings of the International Conference on Artificial Intelligence and Statistics, AISTATS*, pages 249–258, 2016.
- [28] Lam M Nguyen, Jie Liu, Katya Scheinberg, and Martin Takáč. Sarah: A novel method for machine learning problems using stochastic recursive gradient. In *Proceedings of the International Conference on Machine Learning, ICML*, pages 2613–2621, 2017.
- [29] Herbert Robbins and Sutton Monro. A stochastic approximation method. *The Annals of Mathematical Statistics*, 22(3):400–407, 1951.
- [30] Nicol N Schraudolph, Jin Yu, and Simon Günter. A stochastic quasi-newton method for online convex optimization. In *Proceedings of the International Conference on Artificial Intelligence and Statistics AISTATS*, pages 436–443, 2007.
- [31] Damien Scieur, Lewis Liu, Thomas Pumir, and Nicolas Boumal. Generalization of quasi-newton methods: application to robust symmetric multisecant updates. In *Proceedings of the International Conference on Artificial Intelligence and Statistics, AISTATS*, pages 550–558, 2021.
- [32] David F Shanno. Conditioning of quasi-newton methods for function minimization. *Mathematics of computation*, 24(111):647–656, 1970.
- [33] Dinesh Singh, Debaditya Roy, and C. Krishna Mohan. Dip-svm : Distribution preserving kernel support vector machine for big data. *IEEE Transactions on Big Data*, 3(1):79–90, 2017.
- [34] Saeed Soori, Konstantin Mishchenko, Aryan Mokhtari, Maryam Mehri Dehnavi, and Mert Gürbüzbalaban. Dave-qn: A distributed averaged quasi-newton method with local superlinear convergence rate. In *Proceedings of the International Conference on Artificial Intelligence and Statistics, AISTATS*, pages 1965–1976, 2020.
- [35] Minghan Yang, Dong Xu, Hongyu Chen, Zaiwen Wen, and Mengyun Chen. Enhance curvature information by structured stochastic quasi-newton methods. In *IEEE Conference on Computer Vision and Pattern Recognition, CVPR*, pages 10654–10663, 2021.
- [36] Minghan Yang, Dong Xu, Yongfeng Li, Zaiwen Wen, and Mengyun Chen. Structured stochastic quasi-newton methods for large-scale optimization problems. *arXiv e-prints*, pages arXiv–2006, 2020.
- [37] Kai Zhang, Liang Lan, Zhuang Wang, and Fabian Moerchen. Scaling up kernel SVM on limited resources: A low-rank linearization approach. In Neil D. Lawrence and Mark A. Girolami, editors, *Proceedings of the International Conference on Artificial Intelligence and Statistics, AISTATS*, pages 1425–1434, 2012.

A Proofs

A.1 Proof of Lemma 1

Proof. Let $\lambda_1(\mathbf{N}_S), \dots, \lambda_d(\mathbf{N}_S)^\dagger$ are the eigenvalues of the Nystrom approximation $\mathbf{Z}_S \mathbf{Z}_S^T = \mathbf{N}_S$ in the decreasing order; i.e., $\lambda_i(\mathbf{N}_S) \geq \lambda_{i+1}(\mathbf{N}_S)$, for $i \in \{1, \dots, d-1\}$. From the Assumption 4, it is clear that $\gamma \leq \lambda_{\min}(\mathbf{N}_S)$ and $\lambda_{\max} \leq \Gamma$.

Now, using Weyl's theorem [3, Theorem 3.2.1] for the eigenvalues of two symmetric matrices, we prove bound on $\mathbf{N}_S + \rho \mathbf{I}$, for $\rho > 0$.

$$\lambda_i(\mathbf{N}_S) + \lambda_d(\rho \mathbf{I}) \leq \lambda_i(\mathbf{N}_S + \rho \mathbf{I}) \leq \lambda_i(\mathbf{N}_S) + \lambda_1(\rho \mathbf{I}), \text{ for } i \in \{1, \dots, d\},$$

which implies,

$$\lambda_{\min}(\mathbf{N}_S) + \rho \leq \lambda_i(\mathbf{N}_S + \rho \mathbf{I}) \leq \lambda_{\max}(\mathbf{N}_S) + \rho, \text{ for } i \in \{1, \dots, d\}.$$

Therefore,

$$(\gamma + \rho) \mathbf{I} \preceq (\mathbf{N}_S + \rho \mathbf{I}) \preceq (\Gamma + \rho) \mathbf{I}.$$

■

■

A.2 Proof of Lemma 2

Proof. From the Lemma 1, it is easy to see that,

$$\frac{1}{(\Gamma + \rho)} \mathbf{I} \preceq (\mathbf{N}_S + \rho \mathbf{I})^{-1} \preceq \frac{1}{(\gamma + \rho)} \mathbf{I}.$$

Therefore,

$$\frac{1}{(\Gamma + \rho)} \mathbf{I} \preceq \mathbf{B}_S \preceq \frac{1}{(\gamma + \rho)} \mathbf{I}.$$

■

■

[†]For a matrix X , $\lambda(X)$ denotes an eigenvalue of X .

A.3 Proof of Lemma 4

Proof. From the strong convexity of f ,

$$\begin{aligned}
f(\mathbf{z}) &\geq f(\mathbf{w}) + \nabla f(\mathbf{w})^T(\mathbf{z} - \mathbf{w}) + \frac{\mu}{2}\|\mathbf{z} - \mathbf{w}\|^2 \\
&\geq f(\mathbf{w}) + \nabla f(\mathbf{w})^T \left(-\frac{1}{\mu} \nabla f(\mathbf{w}) \right) + \frac{\mu}{2} \left\| \frac{1}{\mu} \nabla f(\mathbf{w}) \right\|^2 \\
&= f(\mathbf{w}) - \frac{1}{2\mu} \|\nabla f(\mathbf{w})\|^2,
\end{aligned} \tag{16}$$

where the last inequality holds from the minimizer $\mathbf{z} = \mathbf{w} - \frac{1}{\mu} \nabla f(\mathbf{w})$ of quadratic model:

$$q(\mathbf{z}) = f(\mathbf{w}) + \nabla f(\mathbf{w})^T(\mathbf{z} - \mathbf{w}) + \frac{\mu}{2}\|\mathbf{z} - \mathbf{w}\|^2.$$

By setting $\mathbf{z} = \mathbf{w}_*$ in (16) gives

$$\|\nabla f(\mathbf{w})\|^2 \geq 2\mu(f(\mathbf{w}) - f(\mathbf{w}_*)).$$

■

■

A.4 Proof of Theorem 2

Proof. Using Assumption 3, we get

$$\begin{aligned}
f(\mathbf{w}_t) &\leq f(\mathbf{w}_{t-1}) + \nabla f(\mathbf{w}_{t-1})^T(\mathbf{w}_t - \mathbf{w}_{t-1}) + \frac{\Lambda}{2}\|\mathbf{w}_t - \mathbf{w}_{t-1}\|^2 \\
&= f(\mathbf{w}_{t-1}) - \eta \nabla f(\mathbf{w}_{t-1})^T \mathbf{B}_\tau \mathbf{v}_{t-1} + \frac{\eta^2 \Lambda}{2} \|\mathbf{B}_\tau \mathbf{v}_{t-1}\|^2.
\end{aligned}$$

Taking expectation on f ,

$$\mathbb{E}[f(\mathbf{w}_t)] \leq f(\mathbf{w}_{t-1}) - \eta \nabla f(\mathbf{w}_{t-1})^T \mathbf{B}_\tau \nabla f(\mathbf{w}_{t-1}) + \frac{\eta^2 \Lambda}{2} \mathbb{E} \|\mathbf{B}_\tau \mathbf{v}_{t-1}\|^2$$

From Lemma 2, we get

$$\mathbb{E}[f(\mathbf{w}_t)] \leq f(\mathbf{w}_{t-1}) - \frac{\eta}{(\Gamma + \rho)} \|\nabla f(\mathbf{w}_{t-1})\|^2 + \frac{\eta^2 \Lambda}{2(\gamma + \rho)^2} \mathbb{E} \|\mathbf{v}_{t-1}\|^2 \tag{17}$$

$$\begin{aligned}
&\leq f(\mathbf{w}_{t-1}) - \frac{2\eta\mu}{(\Gamma + \rho)} (f(\mathbf{w}_{t-1}) - f(\mathbf{w}_*)) \\
&\quad + \frac{2\eta^2 \Lambda^2}{(\gamma + \rho)^2} (f(\mathbf{w}_{t-1}) - f(\mathbf{w}_*) + f(\mathbf{w}_{\tau-1}) - f(\mathbf{w}_*))
\end{aligned} \tag{18}$$

where the last inequality follows from the Lemma 4 and Lemma 3 for the second and the third term, respectively. Now, taking sum over $t = 1, \dots, \ell$, we get

$$\begin{aligned}
\mathbb{E}[f(\mathbf{w}_\ell)] &\leq \mathbb{E}[f(\mathbf{w}_0)] + \frac{2\ell\eta^2\Lambda^2}{(\gamma + \rho)^2} \mathbb{E}[f(\mathbf{w}_{\tau-1}) - f(\mathbf{w}_*)] \\
&\quad - 2\eta \left(\frac{\mu}{(\Gamma + \rho)} - \frac{\eta\Lambda^2}{(\gamma + \rho)^2} \right) \left[\sum_{t=1}^{\ell} f(\mathbf{w}_{t-1}) - \ell f(\mathbf{w}_*) \right] \\
&\leq \mathbb{E}[f(\mathbf{w}_{\tau-1})] + \frac{2\ell\eta^2\Lambda^2}{(\gamma + \rho)^2} \mathbb{E}[f(\mathbf{w}_{\tau-1}) - f(\mathbf{w}_*)] \\
&\quad - 2\eta\ell \left(\frac{\mu}{(\Gamma + \rho)} - \frac{\eta\Lambda^2}{(\gamma + \rho)^2} \right) \mathbb{E}[f(\mathbf{w}_\tau) - f(\mathbf{w}_*)]
\end{aligned}$$

Rearranging above inequality gives

$$\begin{aligned}
0 &\leq \mathbb{E}[f(\mathbf{w}_{\tau-1}) - f(\mathbf{w}_\ell)] + \frac{2\ell\eta^2\Lambda^2}{(\gamma + \rho)^2} \mathbb{E}[f(\mathbf{w}_{\tau-1}) - f(\mathbf{w}_*)] \\
&\quad - 2\eta\ell \left(\frac{\mu}{(\Gamma + \rho)} - \frac{\eta\Lambda^2}{(\gamma + \rho)^2} \right) \mathbb{E}[f(\mathbf{w}_\tau) - f(\mathbf{w}_*)] \\
&\leq \mathbb{E}[f(\mathbf{w}_{\tau-1}) - f(\mathbf{w}_*)] + \frac{2\ell\eta^2\Lambda^2}{(\gamma + \rho)^2} \mathbb{E}[f(\mathbf{w}_{\tau-1}) - f(\mathbf{w}_*)] \\
&\quad - 2\eta\ell \left(\frac{\mu}{(\Gamma + \rho)} - \frac{\eta\Lambda^2}{(\gamma + \rho)^2} \right) \mathbb{E}[f(\mathbf{w}_\tau) - f(\mathbf{w}_*)] \\
&\leq \left(1 + \frac{2\ell\eta^2\Lambda^2}{(\gamma + \rho)^2} \right) \mathbb{E}[f(\mathbf{w}_{\tau-1}) - f(\mathbf{w}_*)] \\
&\quad - 2\eta\ell \left(\frac{\mu}{(\Gamma + \rho)} - \frac{\eta\Lambda^2}{(\gamma + \rho)^2} \right) \mathbb{E}[f(\mathbf{w}_\tau) - f(\mathbf{w}_*)]
\end{aligned}$$

The second inequality follows from the fact that $f(\mathbf{w}_*) \leq f(\mathbf{w}_\ell)$. From the assumption of $\eta < \mu\Delta/2\Lambda^2\delta^2$, which implies

$$\mathbb{E}[f(\mathbf{w}_\tau) - f(\mathbf{w}_*)] \leq \frac{1 + 2\ell\eta^2\Lambda^2\delta^2}{2\ell\eta(\mu\Delta - \eta\Lambda^2\delta^2)} \mathbb{E}[f(\mathbf{w}_{\tau-1}) - f(\mathbf{w}_*)] \quad (19)$$

where,

$$\Delta = \frac{1}{(\Gamma + \rho)}, \quad \delta = \frac{1}{(\gamma + \rho)}$$

Choosing ℓ and η to satisfy (11), it follows that the $\alpha < 1$. ■

A.5 Proof of Theorem 3

Proof. Using Assumption 3, it follows that

$$\begin{aligned}
f(\mathbf{w}_t) &\leq f(\mathbf{w}_{t-1}) + \nabla f(\mathbf{w}_{t-1})^T (\mathbf{w}_t - \mathbf{w}_{t-1}) + \frac{\Lambda}{2} \|\mathbf{w}_t - \mathbf{w}_{t-1}\|^2 \\
&= f(\mathbf{w}_{t-1}) - \eta \nabla f(\mathbf{w}_{t-1})^T \mathbf{B}_\tau \nabla f(\mathbf{w}_{t-1}) + \frac{\eta^2 \Lambda}{2} \|\mathbf{B}_{\tau-1} \nabla f(\mathbf{w}_{t-1})\|^2.
\end{aligned}$$

Taking expectation on f ,

$$\mathbb{E}[f(\mathbf{w}_t)] \leq f(\mathbf{w}_{t-1}) - \frac{\eta}{(\Gamma + \rho)} \|\nabla f(\mathbf{w}_{t-1})\|^2 + \frac{\eta^2 \Lambda}{2} \mathbb{E} \|\mathbf{B}_{\tau-1} \nabla f(\mathbf{w}_{t-1})\|^2$$

From Lemma 4, we get

$$\begin{aligned} \mathbb{E}[f(\mathbf{w}_t)] &\leq f(\mathbf{w}_{t-1}) - \frac{\eta}{(\Gamma + \rho)} \|\nabla f(\mathbf{w}_{t-1})\|^2 + \frac{\eta^2 \Lambda}{2(\gamma + \rho)^2} \mathbb{E} \|\nabla f(\mathbf{w}_{t-1})\|^2 \\ &\leq f(\mathbf{w}_{t-1}) - \frac{2\eta\mu}{(\Gamma + \rho)} (f(\mathbf{w}_{t-1}) - f(\mathbf{w}_*)) + \frac{\eta^2 \Lambda \theta^2}{2(\gamma + \rho)^2} \end{aligned} \quad (20)$$

where the last inequality follows from the Lemma 4 and Assumption 5 for the second and the third term, respectively. Finally adding and subtracting $f(\mathbf{w}_*)$,

$$\begin{aligned} \mathbb{E}[f(\mathbf{w}_t) - f(\mathbf{w}_*)] &\leq f(\mathbf{w}_{t-1}) - f(\mathbf{w}_*) - \frac{2\eta\mu}{(\Gamma + \rho)} (f(\mathbf{w}_{t-1}) - f(\mathbf{w}_*)) + \frac{\eta^2 \Lambda \theta^2}{2(\gamma + \rho)^2} \\ &\leq \left(1 - \frac{2\eta\mu}{(\Gamma + \rho)}\right) (f(\mathbf{w}_{t-1}) - f(\mathbf{w}_*)) + \frac{\eta^2 \Lambda \theta^2}{2(\gamma + \rho)^2}. \end{aligned}$$

Let us define ψ_t be the expectation of $f(\mathbf{w}_t) - f(\mathbf{w}_*)$, over ,

$$\psi_t = \mathbb{E}[f(\mathbf{w}_t) - f(\mathbf{w}_*)].$$

Then,

$$\psi_t \leq \left(1 - \frac{2\eta\mu}{(\Gamma + \rho)}\right) \psi_{t-1} + \frac{\eta^2 \Lambda \theta^2}{2(\gamma + \rho)^2}. \quad (21)$$

Using $\Delta = 1/(\Lambda + \rho)$ and $\delta = 1/(\gamma + \rho)$,

$$\psi_t \leq (1 - 2\eta\mu\Delta) \psi_{t-1} + \frac{\eta^2 \Lambda \theta^2 \delta^2}{2}. \quad (22)$$

Next, we prove the theorem by induction. The above result holds for $t = 1$. Now we assume that it holds for some value of $t > 1$. Since we assume $\eta = \beta/t$, using (22), and (14) we get

$$\begin{aligned} \psi_t &\leq \left(1 - \frac{2\beta\mu\Delta}{t}\right) \frac{g(\beta)}{t} + \frac{\beta^2 \Lambda \theta^2 \delta^2}{2t^2} \\ &= \left(\frac{t-1-2\beta\mu\Delta+1}{t}\right) \frac{g(\beta)}{t} + \frac{\beta^2 \Lambda \theta^2 \delta^2}{2t^2} \\ &= \frac{(t-1)g(\beta)}{t^2} - \frac{(2\beta\mu\Delta-1)g(\beta)}{t^2} + \frac{\beta^2 \Lambda \theta^2 \delta^2}{2t^2} \\ &\leq \frac{g(\beta)}{t+1} \end{aligned}$$

■

■

A.6 Proof of Corollary 1

Proof. Lemma 1 ensures that the approximation satisfies,

$$(\gamma + \rho)\mathbf{I} \preceq (\mathbf{N}_S + \rho\mathbf{I}) \preceq (\Gamma + \rho)\mathbf{I}.$$

Since, step 13 of Algorithm 2 is a special case of (12), the final result follows from Theorem 3. ■ ■

B Additional Results

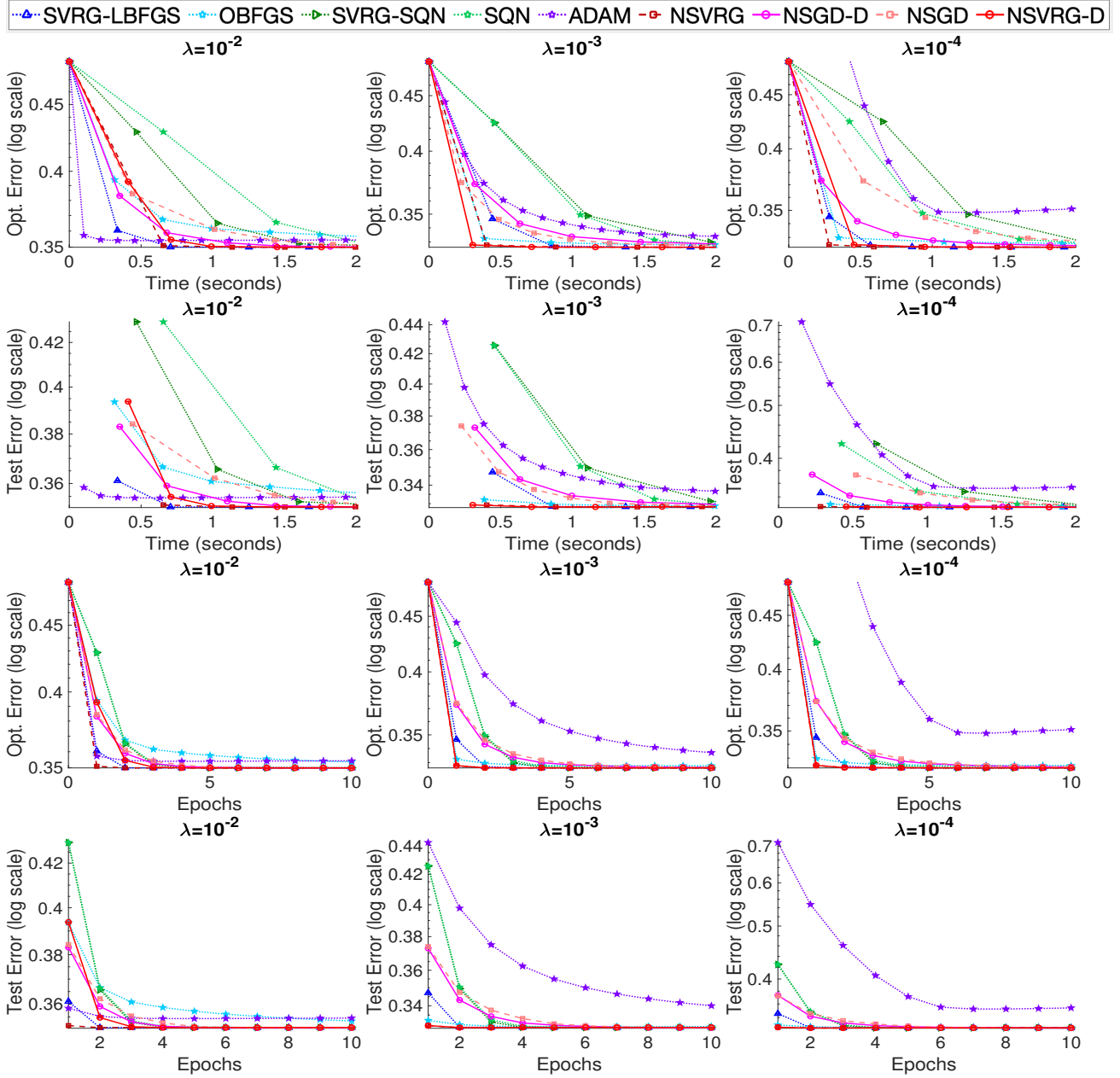


Figure 7: Comparison of proposed methods with the existing optimization methods for optimization performances achieved within 2 seconds on *adult* dataset with various regularizer λ .

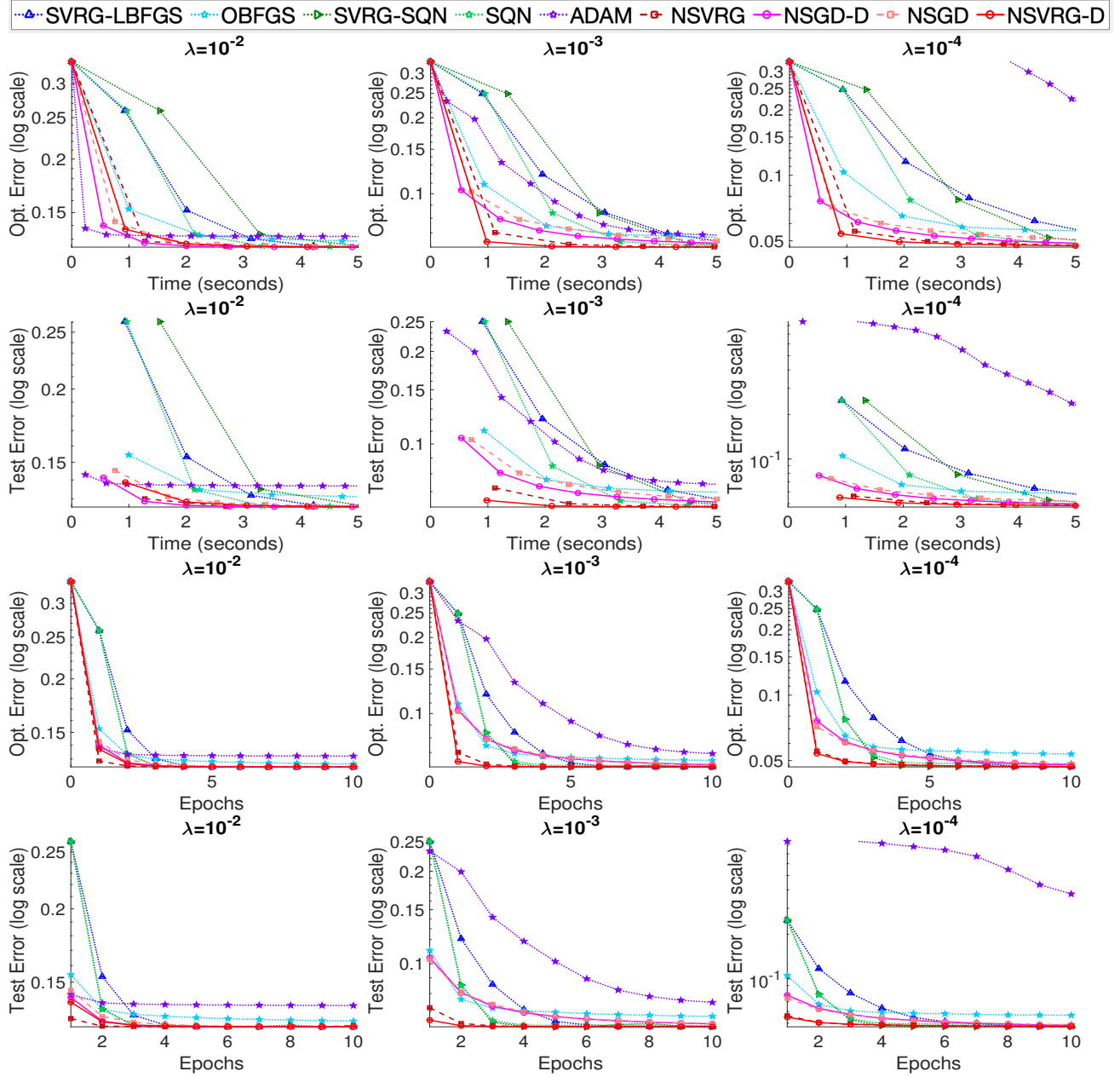


Figure 8: Comparison of proposed methods with the existing optimization methods for optimization performances achieved within 5 seconds on $w8a$ dataset with various regularizer λ .

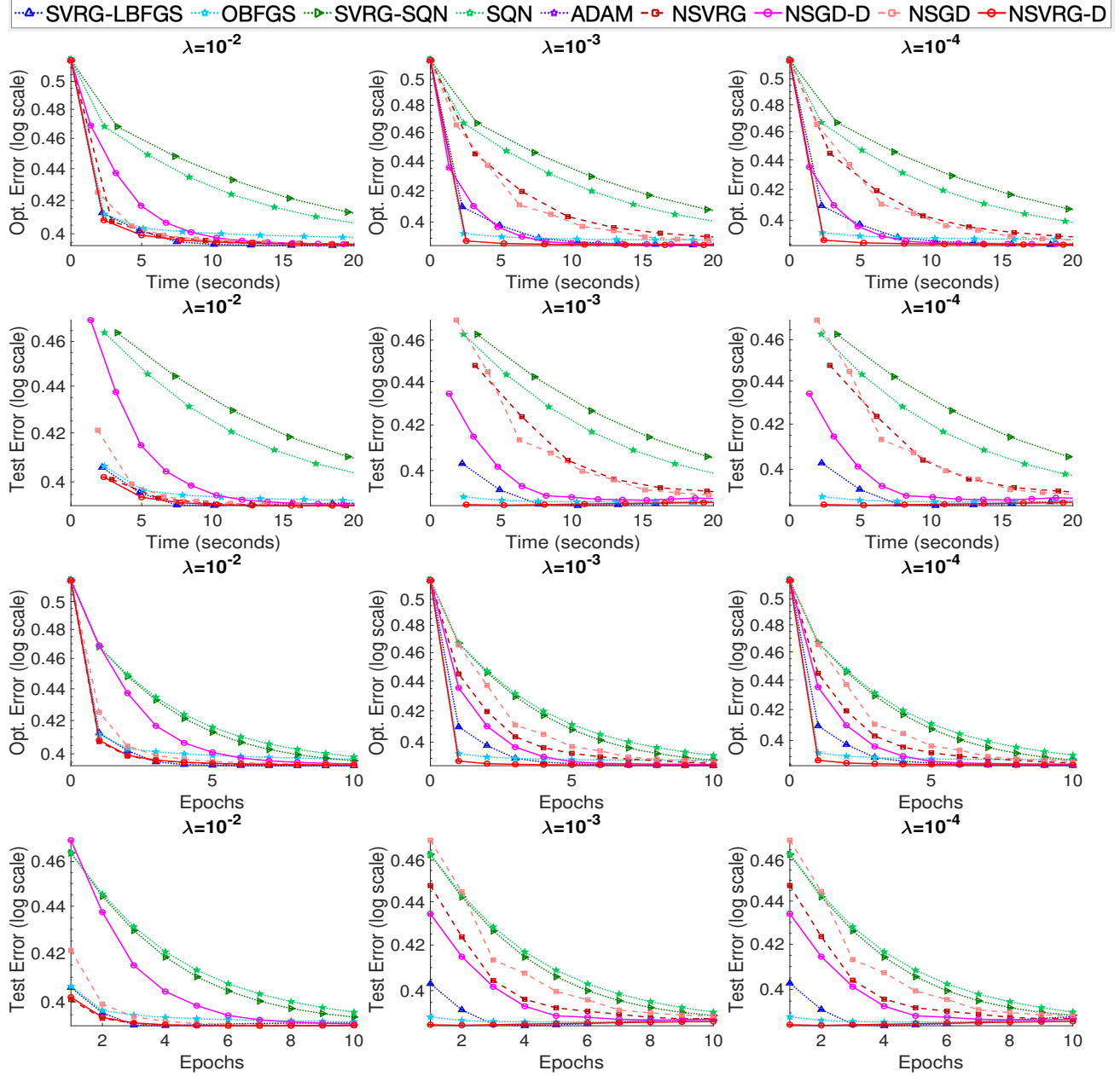


Figure 9: Comparison of proposed methods with the existing optimization methods for optimization performances achieved within 20 seconds on *mnist* dataset with various regularizer λ .

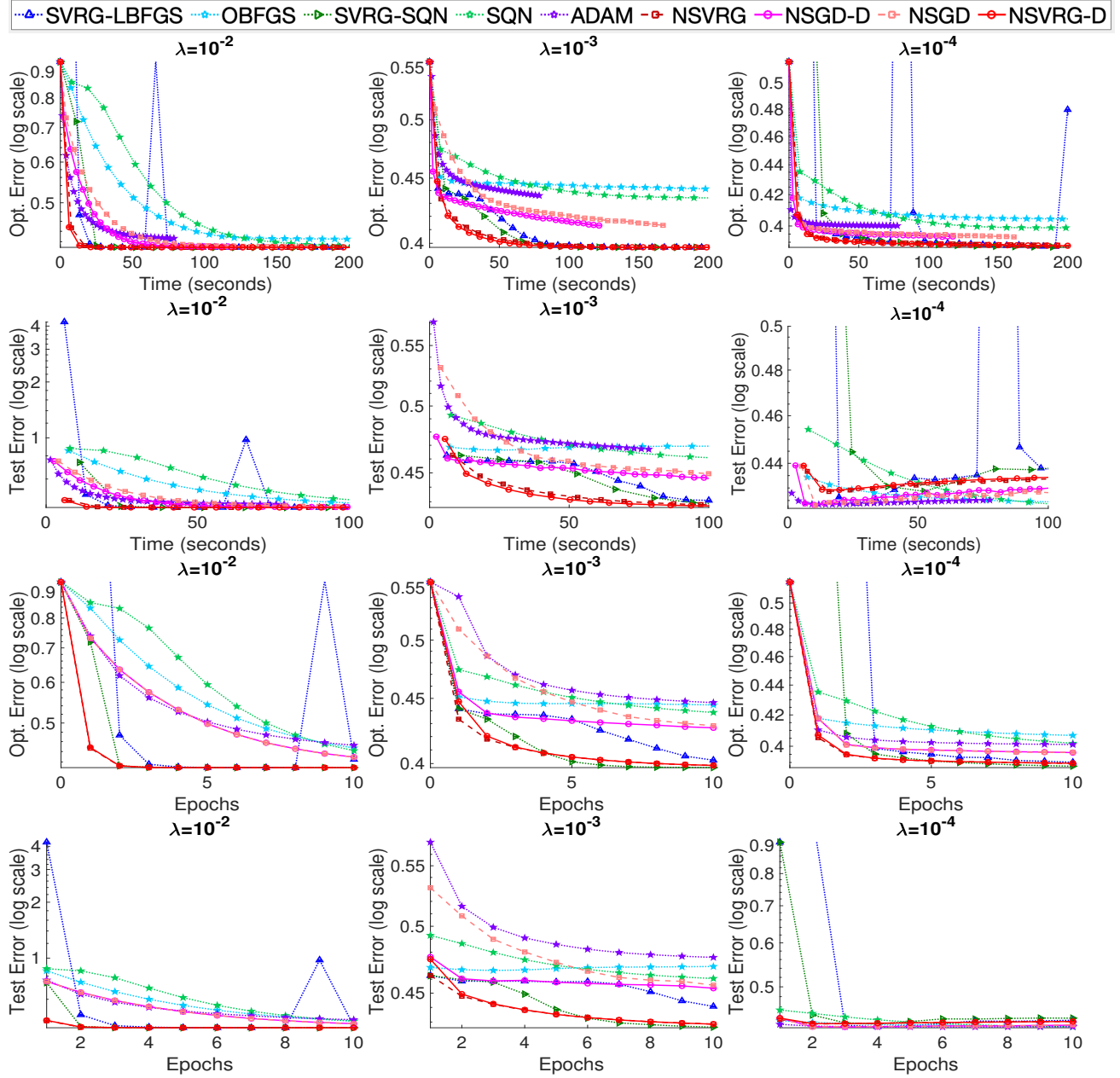


Figure 10: Comparison of proposed methods with the existing optimization methods for optimization performances achieved within 200 seconds on *cifar10* dataset with various regularizer λ .

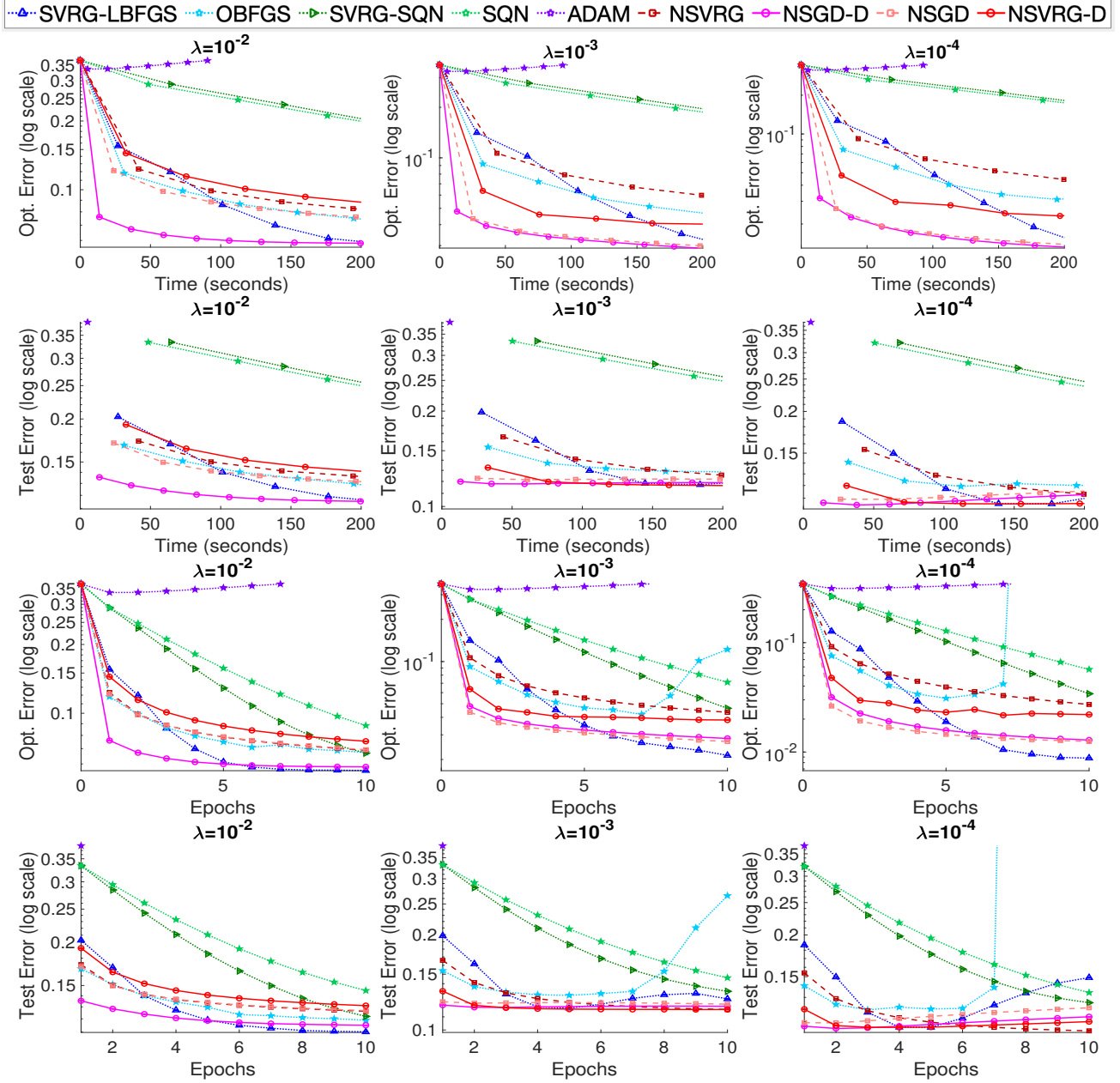


Figure 11: Comparison of proposed methods with the existing optimization methods for optimization performances achieved within 200 seconds on *real-sim* dataset with various regularizer λ .

C DP sub-sampling

Algorithm 3 Distribution-Preserving Sub-sampling

Parameters: Number of subsets P and number of clusters K

```

1:  $\mathbf{X}^+ \leftarrow \{\mathbf{x}_i | y_i = 1\}_{i=1}^n$ 
2:  $\mathbf{X}^- \leftarrow \{\mathbf{x}_i | y_i = -1\}_{i=1}^n$ 
3:  $\{\mathbf{X}_1^+, \dots, \mathbf{X}_K^+\} \leftarrow \text{kmeans}(\mathbf{X}^+, K)$ 
4:  $\{\mathbf{X}_1^-, \dots, \mathbf{X}_K^-\} \leftarrow \text{kmeans}(\mathbf{X}^-, K)$ 
5: for  $k = 1 \rightarrow K$  do
6:    $\{\mathbf{X}_{k,1}^+, \dots, \mathbf{X}_{k,P}^+\} \leftarrow \text{uniform\_split}(\mathbf{X}_k^+, P)$ 
7:    $\{\mathbf{X}_{k,1}^-, \dots, \mathbf{X}_{k,P}^-\} \leftarrow \text{uniform\_split}(\mathbf{X}_k^-, P)$ 
8:   for  $p = 1 \rightarrow P$  do
9:      $\mathbf{X}_p \leftarrow \mathbf{X}_p \cup \mathbf{X}_{k,p}^+ \cup \mathbf{X}_{k,p}^-$ 
10:     $\mathbf{y}_p \leftarrow \mathbf{y}_p \cup \mathbf{1}^{|\mathbf{X}_{k,p}^+|} \cup -\mathbf{1}^{|\mathbf{X}_{k,p}^-|}$ 
11:   end for
12: end for
13: return  $\{\mathcal{S}_p = (\mathbf{X}_p, \mathbf{y}_p)\}_{p=1}^P$ 

```
